Available online at www.sciencedirect.com
SCIENCE DIRECT®
Journal of Solid State Chemistry 177 (2004) 4112–4118
JOURNAL OF SOLID STATE CHEMISTRY
http://elsevier.com/locate/jssc

Chemical stability of $La_{1-x}Sr_xCrO_3$ in oxidizing atmospheres

Shogo Miyoshi,[a,*] Shigenori Onuma,[a] Atsushi Kaimai,[a] Hiroshige Matsumoto,[a] Keiji Yashiro,[a] Tatsuya Kawada,[a] Junichiro Mizusaki,[a] and Harumi Yokokawa[b]

[a] *Institute of Multidisciplinary Research for Advanced Materials, Tohoku University, 2-1-1 Katahira, Aoba-ku, Sendai 980-8577, Japan*
[b] *National Institute of Advanced Industrial Science and Technology, 1-1-1 Higashi, Tsukuba 305-8565, Japan*

Received 8 January 2004; received in revised form 25 April 2004; accepted 30 April 2004

Available online 6 October 2004

Abstract

The single-phase region of $La_{1-x}Sr_xCrO_3$ ($x = 0.1$, 0.2, 0.3) was precisely determined as a function of temperature, P_{O_2} and Sr content. The powders with the nominal composition of $La_{1-x}Sr_xCrO_3$ were equilibrated under various conditions, and then identified by XRD analyses. To confirm the equilibration, two independent experiments were performed for each composition observing (i) the precipitation of the second phase from a single-phase solid solution, and (ii) the formation of the single phase from the constituent oxides. Two kinds of second phases, $SrCrO_4$ and an unknown phase, were observed depending on the conditions. The second phases tended to appear at low temperature, in high P_{O_2} and with a large Sr content. The single-phase regions obtained via the two equilibration routes were in good agreement with each other. The thermodynamic calculations on the supposition of ideality of the solid solution essentially reproduced the experimental results. When this material is used as the interconnects of solid oxide fuel cells, much attention should be paid to its relatively narrow solubility range of Sr; for example, the solubility limit is approximately 0.1 under a typical cathode-side condition (1273 K, air).
© 2004 Elsevier Inc. All rights reserved.

Keywords: $La_{1-x}Sr_xCrO_3$; Perovskite; Chemical stability; Solubility limit; Solid oxide fuel cell; Interconnector

1. Introduction

A series of perovskite-type doped $LaCrO_3$ has attracted much attention as an interconnector material of solid oxide fuel cells (SOFCs) which operate at high temperatures such as 1273 K. Also, these oxides have recently been considered as an alternative to the Ni-YSZ anodes in the SOFCs fueled with hydrocarbons [1–3]. Lanthanum chromites have an excellent tolerance for reducing environments, which particularly motivates us to apply them to the interconnectors and anodes of SOFCs. On the other hand, it is expected that the solubility limit of dopants decreases under oxidizing atmospheres, and the second phase precipitates [4–8]. The formation of the second phase can produce serious problems such as the degradation of the electronic conductivity and the mechanical properties. Moreover, the second phase may react with the other SOFC components to yield undesirable compounds [9].

For $La_{1-x}M_xCrO_3$ (M = Ca, Sr), several phase studies have been carried out [4–8]. The second phase which appears in oxidizing atmospheres was identified as $MCrO_4$ by Carter et al. [4] and Peck et al. [5,6]; the Cr ion in the compound is hexavalent. In addition, they also determined the solubility limit of alkaline earths in air; for example, $x = 0.3$ at 1273 K and $x = 0.2$ at 1173 K for Ca [4], and $x = 0.10$ at 1223 K for Sr [6]. The thermodynamic calculation performed by Yokokawa et al. also predicted the segregation of $MCrO_4$ [7].

In all the phase studies mentioned above, the experiments were done only under atmospheric conditions; that is, the concerned oxygen partial pressure is limited to 0.21 bar. Since the phase precipitation of $MCrO_4$ from the solid solution involves the oxidation of the Cr ion, the solubility limit of the alkaline earth must depend on the temperature and ambient oxygen partial pressure, P_{O_2}. Furthermore, the operating conditions of the SOFCs vary in temperature and P_{O_2}. The reason for

*Corresponding author. Present address: Department of Applied Chemistry, Faculty of Engineering, Kyushu University, 6-10-1 Hakozaki, Higashi-ku, Fukuoka 812-8581, Japan. Fax: +81-92-651-5606.
E-mail address: miyoshi@cstf.kyushu-u.ac.jp (S. Miyoshi).

0022-4596/$ - see front matter © 2004 Elsevier Inc. All rights reserved.
doi:10.1016/j.jssc.2004.04.054

the variability of P_{O_2} is that in the pressurized systems, the total pressure in the cathode side is as high as several bars; consequently, the P_{O_2} is higher than 0.21 bar. Therefore, it is necessary to understand the phase relationship as a function of the dopant content, temperature and P_{O_2}. In a preceding study, we obtained the detailed phase relationship of $La_{1-x}Ca_xCrO_3$ in high P_{O_2} [8]. We employed two independent experimental methods which undergo the dissolution and precipitation of the second phase, respectively. The single-phase regions obtained by both methods agreed with each other, indicating that the results well reproduce the true phase equilibria.

The present study aims to determine the precise and accurate single-phase regions of $La_{1-x}Sr_xCrO_3$ in oxidizing atmospheres. The powders with the nominal composition of $La_{1-x}Sr_xCrO_3$ ($x = 0.1$, 0.2, 0.3) were equilibrated under various conditions of temperature and P_{O_2}, and then identified by XRD analyses. Similar to our previous study mentioned above, we performed the two patterns of equilibration as follows and illustrated in Fig. 1: the dissolution and precipitation of the second phase.

In the dissolution experiment, the powders as synthesized via a solution process were directly equilibrated under controlled temperatures and P_{O_2}'s (Fig. 1(a)), followed by XRD analyses. Since the syntheses were performed at relatively low temperatures, the as-synthesized powders consisted of the perovskite phase and the second phase including Sr. During the equilibration at a temperature higher than that for the synthesis, the second phase dissolves into the perovskite phase [10]. The dissolution proceeds until the Sr content in the solid solution reaches the solubility limit or the second phase disappears. In this way, we examined whether the second phase completely dissolves under various conditions.

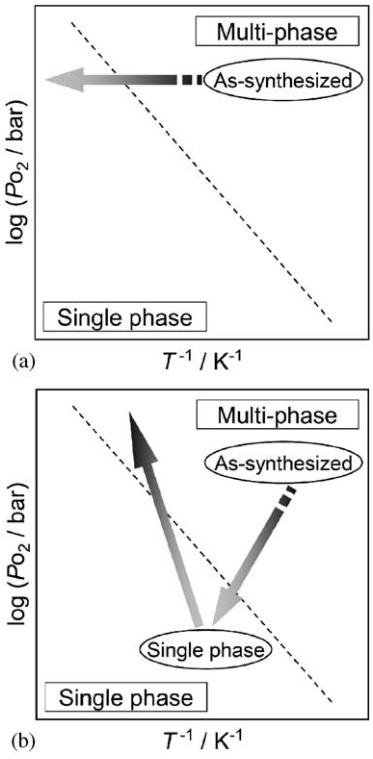

Fig. 1. Schematics of the two patterns of equilibration: (a) the dissolution experiment; (b) the precipitation experiment. The routes of each experiment are shown in typical phase diagrams. The broken lines denote the boundaries between the single- and multi-phase regions.

With regard to the precipitation experiment (Fig. 1(b)), the as-synthesized powders were first equilibrated under the presumed single-phase conditions. The obtained single-phase powders were subsequently equilibrated under various conditions in order to observe whether the second phase precipitates from the single-phase solid solution. In the first equilibration for the single-phase preparation, we set the temperature as low as possible so as to prevent severe grain growth. If the starting single-phase sample has large grain size due to a very high-temperature treatment, the phase separation is expected to take a very long time, or the equilibrium may not be attained in a practical period of time.

Both of the experiments are complementary to each other. Since the dissolution and precipitation of the second phase are regarded as a solid-state reaction with slow kinetics, it is possible that the ideal equilibrium is not attained at the end of the equilibration. If this is the case, the dissolution experiment and precipitation experiment tend to give smaller and larger single-phase regions than the true one, respectively. In this context, the single-phase regions obtained with the two equilibration processes will be compared to each other in order to discuss the reliability. Also, the stable phase(s) under various conditions were evaluated with thermodynamic calculations using the program SOLGASMIX [11] in combination with the thermochemical database CTC [12].

2. Experimental

2.1. Sample preparation

The powders with the nominal composition of $La_{1-x}Sr_xCrO_3$ ($x = 0.1$, 0.2, 0.3) were synthesized via a simplified Pechini method [13]. The nitrate solutions of the respective cations were prepared by dissolving La_2O_3 and $SrCO_3$ with diluted HNO_3, and $Cr(NO_3)_2 \cdot 9H_2O$ into distilled water. The concentration of the cation in each nitrate solution was determined by a chelate titration. The nitrate solutions were mixed together in the appropriate ratios, followed by addition of citric acid of three times the total molar number of the cations. The mixed solutions were well stirred, and then heated to about 800 K in order to be dried and burned

into ash-like solids. The obtained products were ground into powders with a mortar. XRD analyses with Cu$K\alpha$ radiation (RAD IR, RIGAKU) showed that the as-synthesized powders consisted of a perovskite phase and the other phases.

2.2. Dissolution experiment

The as-synthesized powders were directly equilibrated under various conditions of temperature (1073–1473 K) and P_{O_2} (10^{-3}–1 bar) as follows. About 0.1 g of the as-synthesized powder was put into a platinum vessel, and rapidly heated to the programmed temperature. No compression was applied to the powder before the equilibration for the following reason. The employed synthesis method was not a conventional powder mixing process but the simplified Pechini method, which offers high homogeneity of cationic composition from the stage of mixed nitrate solution. It is therefore considered that, cation migration beyond the grain size of the fine as-synthesized powder is not necessary to obtain the single-phase through the equilibration; thus, the experiment was performed using loose powder. The sample was kept at the programmed temperature for 100 h, and subsequently cooled to room temperature taking less than 15 min. Throughout the equilibration procedure, the ambient P_{O_2} was regulated by the gas mixture flow of O_2–N_2. The obtained powder was identified by XRD analysis to examine whether the second phase completely dissolved into the perovskite phase under the stated conditions.

2.3. Precipitation experiment

In a way identical to the dissolution experiment, the as-synthesized powders were first equilibrated to prepare the single-phase of the solid solution. The conditions for the first equilibration were selected based on the results of the dissolution experiment as follows: for $x = 0.1$, 1123 K and $P_{O_2} = 10^{-5}$ bar; for $x = 0.2$, 1198 K and $P_{O_2} = 10^{-3}$ bar; and for $x = 0.3$, 1298 K and $P_{O_2} = 10^{-2}$ bar. The XRD analyses confirmed that the prepared powders after the initial equilibration consisted of the single-phase solid solution. The single-phase powders were then equilibrated again under the other conditions which are close to the boundary between the single-phase region and the multi-phase region. The obtained powders were analyzed by XRD to observe whether the second phase precipitated under the stated conditions.

2.4. Thermodynamic calculation

The stable phase(s) under various conditions (P_{O_2}, temperature and Sr content) were evaluated using a thermodynamic calculation program, SOLGASMIX [11], which finds the equilibrium state that minimizes the overall Gibbs energy in the system. In this evaluation, the *A*-site substituted lanthanum chromite, (La,Sr)CrO_3, was assumed to be an ideal solution of the constituent perovskites, $LaCrO_3$ and $SrCrO_3$. The thermodynamic data for the compounds were taken from the thermodynamic database CTC [12], or estimated as reported in the literature [7].

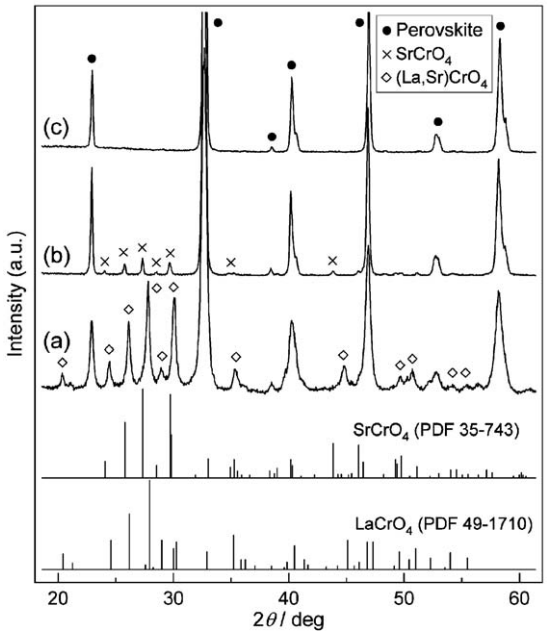

Fig. 2. Typical XRD patterns (Cu$K\alpha$) obtained by the dissolution experiment. The nominal composition of the sample is $La_{0.8}Sr_{0.2}CrO_3$: (a) as-synthesized via a simplified Pechini method; (b) and (c) equilibrated in $P_{O_2} = 10^{-2}$ bar at 1173 and 1223 K, respectively.

3. Results and discussion

3.1. Dissolution experiment

Fig. 2 shows typical XRD patterns of the as-synthesized and equilibrated powders with the nominal composition of $La_{0.8}Sr_{0.2}CrO_3$. The pattern (a) resulted from the as-synthesized powder, showing the coexistence of the perovskite phase and the second phase. The peaks from the second phase in the as-synthesized powder were well indexed as $LaCrO_4$. If the second phase is pure $LaCrO_4$, all of the Sr must have dissolved into the perovskite phase. However, such a situation seems impossible since the dissolution of an alkaline earth is known to be completed at rather high temperatures [10]; the maximum temperature which the as-synthesized powder had experienced was ca. 800 K. Here, $LaCrO_4$ crystallizes in the space group identical with $SrCrO_4$, $P21/n$.[1] Though they give closely

[1] PDF card 49-1710 and 35-743.

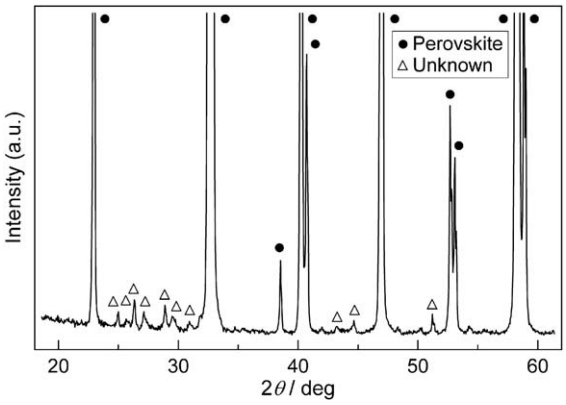

Fig. 3. A typical XRD pattern (Cu$K\alpha$) of the sample including the unknown phase. The nominal composition of the sample is $La_{0.8}Sr_{0.2}CrO_3$. The sample was obtained by the equilibration in $P_{O_2} = 1$ bar at 1423 K.

similar XRD patterns, the unit cell of $SrCrO_4$ is significantly larger than $LaCrO_4$. The Bragg angles of the second phase in the pattern (a) of Fig. 2 were close to those of $LaCrO_4$ rather than $SrCrO_4$. Considering these situations, the second phase in the as-synthesized powder was possibly a solid solution of $LaCrO_4$ and $SrCrO_4$.

The patterns (b) and (c) in Fig. 2 came from the powders which were equilibrated in $P_{O_2} = 10^{-2}$ bar at 1173 and 1223 K, respectively. After the equilibration at 1173 K, the perovskite phase still coexisted with the second phase which was exactly identified as $SrCrO_4$; the existence of $SrCrO_4$ as the second phase of $La_{1-x}Sr_xCrO_3$ agrees with the literature [6]. On the other hand, the equilibration at 1223 K results in complete dissolution of the second phase into the solid solution.

Under some conditions, the second phase other than $SrCrO_4$ was also observed as shown in Fig. 3. Based on a search of the databases and literature, the peaks from such second phase were not assigned to any known compounds. The unknown phase appeared under relatively high P_{O_2} in the powders of $x = 0.2$ and 0.3.

The phase relationship of $La_{1-x}Sr_xCrO_3$ ($x = 0.1, 0.2, 0.3$) obtained from the dissolution experiment is shown in Fig. 4(a)–(c) as a function of temperature and P_{O_2}. In this figure, the open circles (○), diagonal crosses (×) and triangles (△) represent the conditions of the single phase, coexistence with $SrCrO_4$, and coexistence with the unknown phase, respectively. The second phases tended to survive in high P_{O_2}, at low temperature and with a large Sr content.

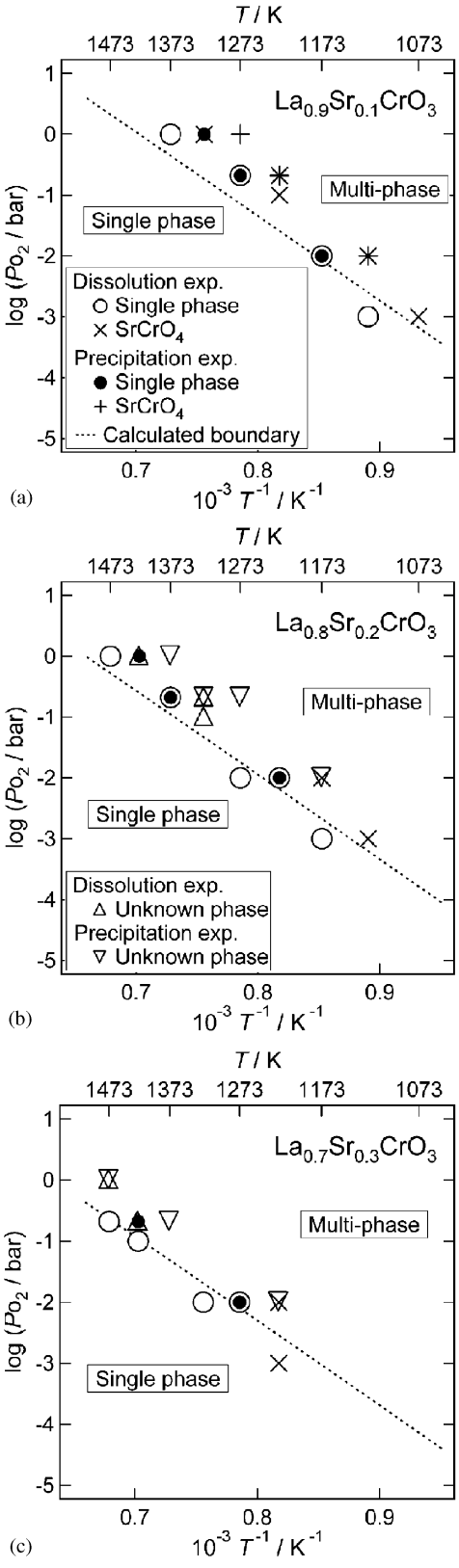

Fig. 4. Phase relationships of $La_{1-x}Sr_xCrO_3$ in oxidizing atmospheres: (a) $x = 0.1$; (b) $x = 0.2$; (c) $x = 0.3$. The symbols: (○), (×) and (△) represent the single phase, coexistence with $SrCrO_4$ and coexistence with the unknown phase in the results of the dissolution experiment, respectively. The symbols: (●), (+) and (▽) represent the single phase, coexistence with $SrCrO_4$ and coexistence with the unknown phase in the results of the precipitation experiment, respectively. The dotted lines represent the phase boundaries obtained from the thermodynamic calculations (Eq. (7)).

3.2. Precipitation experiment

In this experiment, we equilibrated the powders of the single-phase $La_{1-x}Sr_xCrO_3$ ($x = 0.1$, 0.2, 0.3) under various conditions, and observed whether the second phase precipitates from the solid solution during the equilibration (see Fig. 1(b)). The bottom XRD pattern in Fig. 5 shows the single phase of $La_{0.9}Sr_{0.1}CrO_3$, which was obtained by the first equilibration at 1123 K in $P_{O_2} = 10^{-5}$ bar. The middle and upper XRD patterns in Fig. 5 resulted from the second equilibration of the single-phase powder at 1273 K in $P_{O_2} = 0.21$ and 1 bar, respectively. After the second equilibration in $P_{O_2} = 0.21$ bar, the sample still remained as a single phase, whereas the second equilibration in $P_{O_2} = 1$ bar resulted in the precipitation of the second phase, $SrCrO_4$. The unknown phase, which is identical to that observed in the dissolution experiment, was observed as the second phase under some conditions when $x = 0.2$ and 0.3.

In this way, we examined whether the second phase precipitates under various conditions. The obtained phase relationship is also shown in Fig. 4(a)–(c) as a function of temperature and P_{O_2}. In this figure, the closed circles (●), crosses (+) and inverted triangles (▽) represent the conditions of the single phase, coexistence with $SrCrO_4$ and coexistence with the unknown phase, respectively, from the results of the precipitation experiment.

Comparing the results of the precipitation experiments with those of the dissolution experiments shown in Fig. 4, the single-phase regions obtained by both methods were in good agreement with each other. As mentioned before, the precipitation experiment and the dissolution experiment started with the single-phase solid solution and the mixture including the second phase, respectively. Therefore, the former and the latter tend to give the larger and the smaller single-phase regions than the true one due to a kinetic reason, respectively. In reality, the results of both experiments almost agreed with each other. This agreement confirms that the obtained phase relationship well reflects the phase equilibria.

Peck et al. [6] experimentally determined the solubility limit of Sr in $LaCrO_3$ to be $x = 0.10$ at 1223 K in air. The present experimental results are nearly consistent with the reported value. In a close comparison, however, the reported solubility limit is slightly higher than that obtained in this study. In their experiment, the sample was first heat-treated at a rather high temperature such as 1673 K to become a single-phase solid solution, and then annealed at 1223 K. Therefore, it is possible that the equilibrium was not attained at the end of their annealing due to large grain size resulted from the high-temperature pretreatment. This results in the over-estimation of the single-phase region.

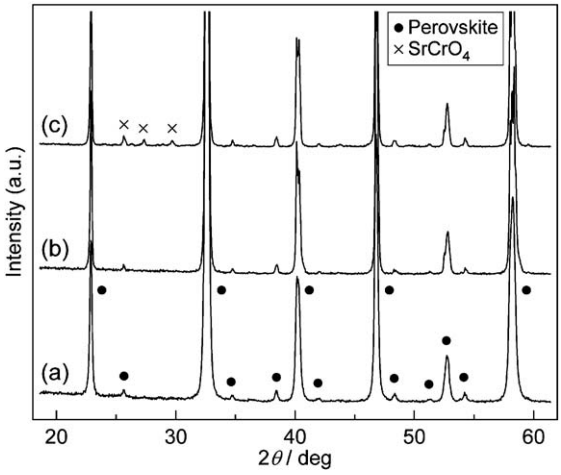

Fig. 5. Typical XRD patterns (Cu$K\alpha$) obtained by the precipitation experiment. The nominal composition of the sample is $La_{0.9}Sr_{0.1}CrO_3$: (a) obtained by the first equilibration in $P_{O_2} = 10^{-5}$ bar at 1123 K; (b) and (c) obtained after the second equilibration at 1273 K in $P_{O_2} = 0.21$ and 1 bar, respectively.

In our previous study [8], the single-phase region of Ca-doped $LaCrO_3$ was also determined. Compared to $La_{1-x}Ca_xCrO_3$, the single-phase region of $La_{1-x}Sr_xCrO_3$ in oxidizing atmospheres is narrow. For example, the solubility limit under a typical cathode condition of an operating SOFC (1273 K, air) is approximately 0.3 for $La_{1-x}Ca_xCrO_3$ while it is about 0.1 for Sr-doping.

However, it should be also noted that there is a difference in the property between the second phases of $La_{1-x}Ca_xCrO_3$ and $La_{1-x}Sr_xCrO_3$. The second phase of $La_{1-x}Ca_xCrO_3$ is exclusively $CaCrO_4$ [4,5,8], which decomposes into $Ca_3(CrO_4)_2$ and some liquid phase at 1334 K [14]. The existence of liquid phase significantly promotes the material transport. This facilitates rapid sintering [15] on the one hand and easy attainment of phase equilibrium on the other. In other words, when $La_{1-x}Ca_xCrO_3$ is placed out of the single-phase conditions, the second phase will rapidly precipitate. In contrast, $SrCrO_4$, the main second phase of $La_{1-x}Sr_xCrO_3$, is more refractory than $CaCrO_4$; the decomposition temperature of $SrCrO_4$ is 1524 K [16]. The precipitation of $SrCrO_4$ from $La_{1-x}Sr_xCrO_3$ is therefore considered as very slow around the typical operation temperature of SOFCs such as 1273 K.

In addition, the difference in the equilibration kinetics was actually inferred in the series of our study, though the concerned temperatures were mostly below the melting temperatures of the second phases. For $La_{1-x}Ca_xCrO_3$, the equilibration for a period of 10 h was enough to obtain the reasonable results [8]. On the other hand, the phase relationships of $La_{1-x}Sr_xCrO_3$ obtained after 10 h and 100 h equilibrations were

different, indicating that the equilibria were not attained after 10 h (in this paper, the results only from 100 h equilibration are described).

Thus $La_{1-x}Sr_xCrO_3$ is considered to possess the kinetic barrier against the precipitation of the second phase, whereas the equilibrium single-phase region of $La_{1-x}Ca_xCrO_3$ is larger than that of $La_{1-x}Sr_xCrO_3$. Perhaps the single phase of $La_{1-x}Sr_xCrO_3$ prepared at high temperatures remains metastable even under the multi-phase conditions, if the oxide is densely sintered with sufficient grain growth. Therefore, it is not simply concluded only from the equilibrium solubility range that $La_{1-x}Ca_xCrO_3$ is superior in the point of chemical stability in oxidizing environments. For the application of $La_{1-x}Sr_xCrO_3$, it is necessary to avoid the contact of the interconnector with any liquid phase in order to maintain the kinetic barrier.

3.3. Thermodynamic calculation

Setting the solid solution $La_{1-x}Sr_xCrO_3$ ($x = 0.1$, 0.2, 0.3) as the starting compositions, the stable compound(s) under various conditions were evaluated with SOLGASMIX/CTC, of which the results are shown in Table 1. This evaluation also suggests the formation of the second phase at low temperatures, in high P_{O_2} and with large Sr content. The major second phase is $SrCrO_4$, whereas a very small amount (0.02% in molar ratio to the entirety at most) of $La_{16}Cr_7O_{44}$ was also predicted for some conditions. For example, 3.5×10^{-2} mol of $SrCrO_4$ and 1.6×10^{-4} mol of $La_{16}Cr_7O_{44}$ precipitates from 1 mol of $La_{0.9}Sr_{0.1}CrO_3$ at 1373 K in $P_{O_2} = 1$ bar.

In the experiments, the XRD did not detect $La_{16}Cr_7O_{44}$. This indicates that even if $La_{16}Cr_7O_{44}$ is stable as the second phase, the quantity is too small to be detectable in XRD analyses. Since the precipitation of $La_{16}Cr_7O_{44}$ from the solid solution is accompanied by the formation of *A*-site vacancies, the present results also suggest the absence of *A*-site vacancies in $La_{1-x}Sr_xCrO_3$.

Since the latter second phase, $La_{16}Cr_7O_{44}$, is the minority, the thermodynamic evaluation practically suggests that the second phase is only $SrCrO_4$. Based on this supposition, we can obtain the detailed phase boundary with a simple thermodynamic calculation as follows. The precipitation of $SrCrO_4$ is regarded as the oxidation of $SrCrO_3$ in the solid solution:

$$SrCrO_3(\text{in solid solution}) + \tfrac{1}{2}O_2 \leftrightarrow SrCrO_4. \quad (1)$$

When the thermodynamic condition corresponds to the boundary between the single-phase and multi-phase regions, the reaction is in equilibrium:

$$\mu(SrCrO_3,\ \text{in s.s.}) + \tfrac{1}{2}\mu(O_2) = \mu(SrCrO_4), \quad (2)$$

where μ denotes the chemical potential of each chemical species. Assuming $La_{1-x}Sr_xCrO_3$ as an ideal solid solution, the chemical potential of $SrCrO_3$ in the solid solution is represented as

$$\mu(SrCrO_3,\ \text{in s.s.}) = \mu^\circ(SrCrO_3) + RT\ln x. \quad (3)$$

Since the standard pressure, P°, is defined as 1.01325 bar in the thermodynamic database [12], the chemical potential of gaseous oxygen is represented with P_{O_2} (bar) as follows:

$$\begin{aligned}\mu(O_2) &= \mu^\circ(O_2) + RT\ln(P_{O_2}/P^\circ)\\ &\cong \mu^\circ(O_2) + RT\ln P_{O_2}.\end{aligned} \quad (4)$$

The following equation holds between standard Gibbs energy of formation and the constituent chemical potentials:

$$\begin{aligned}\Delta_f G^\circ(SrCrO_3) = \mu^\circ(SrCrO_3)\\ - [\mu^\circ(Sr) + \mu^\circ(Cr) + \tfrac{3}{2}\mu^\circ(O_2)],\end{aligned} \quad (5)$$

Table 1
The second phases of $La_{1-x}Sr_xCrO_3$ evaluated using the thermodynamic computation system, SOLGASMIX/CTC

Initial composition	$\log(P_{O_2}/\text{bar})$	T (K)			
		1373	1273	1173	1073
$La_{0.9}Sr_{0.1}CrO_3$	0	$SrCrO_4$, $La_{16}Cr_7O_{44}$	$SrCrO_4$, $La_{16}Cr_7O_{44}$	$SrCrO_4$, $La_{16}Cr_7O_{44}$	$SrCrO_4$, $La_{16}Cr_7O_{44}$
	−1	SP	$SrCrO_4$	$SrCrO_4$	$SrCrO_4$
	−2	SP	SP	$SrCrO_4$	$SrCrO_4$
	−3	SP	SP	SP	$SrCrO_4$
$La_{0.8}Sr_{0.2}CrO_3$	0	$SrCrO_4$, $La_{16}Cr_7O_{44}$	$SrCrO_4$, $La_{16}Cr_7O_{44}$	$SrCrO_4$, $La_{16}Cr_7O_{44}$	$SrCrO_4$, $La_{16}Cr_7O_{44}$
	−1	SP	$SrCrO_4$	$SrCrO_4$	$SrCrO_4$
	−2	SP	SP	$SrCrO_4$	$SrCrO_4$
	−3	SP	SP	SP	$SrCrO_4$
$La_{0.7}Sr_{0.3}CrO_3$	0	$SrCrO_4$, $La_{16}Cr_7O_{44}$	$SrCrO_4$, $La_{16}Cr_7O_{44}$	$SrCrO_4$, $La_{16}Cr_7O_{44}$	$SrCrO_4$, $La_{16}Cr_7O_{44}$
	−1	$SrCrO_4$	$SrCrO_4$	$SrCrO_4$	$SrCrO_4$
	−2	SP	$SrCrO_4$	$SrCrO_4$	$SrCrO_4$
	−3	SP	SP	$SrCrO_4$	$SrCrO_4$

SP: Single phase of perovskite.

$$\Delta_f G^\circ(SrCrO_4) = \mu^\circ(SrCrO_4) - [\mu^\circ(Sr) + \mu^\circ(Cr) + 2\mu^\circ(O_2)]. \quad (6)$$

From Eqs. (2)–(6), the equilibrium condition for reaction (1) is given as

$$\frac{2.303R}{2}\log P_{O_2} = [\Delta_f H^\circ(SrCrO_4) - \Delta_f H^\circ(SrCrO_3)]\frac{1}{T} - [\Delta_f S^\circ(SrCrO_4) - \Delta_f S^\circ(SrCrO_3)] - R\ln x. \quad (7)$$

The thermodynamic functions in Eq. (7) were calculated from those at 298.15 K and the temperature dependence of the specific heat at a constant pressure, which were taken from the database [12]. From the above, the equilibrium condition is derived as a function of T, P_{O_2} and the doping level, x. The phase boundaries thus calculated for $x = 0.1$, 0.2 and 0.3 are shown in Fig. 4(a)–(c) with dotted lines.

The phase boundary obtained by the thermodynamic calculation (Eq. (7)) almost agreed with the experimental results as shown in Fig. 4. This indicates that the precipitation of the second phase is well understood as the oxidation of Cr^{4+} in the solid solution to the higher valence. For $x = 0.2$ and 0.3, the second phase under some conditions was the unknown compound, which is not taken into account in the thermodynamic calculation. Nevertheless, the agreement between the results of the experiments and thermodynamic calculation also holds for $x = 0.2$ and 0.3. Therefore, the unknown phase is regarded as quite close to $SrCrO_4$ in the point of thermodynamic properties.

4. Conclusions

The single-phase region of $La_{1-x}Sr_xCrO_3$ in oxidizing environments was precisely determined as a function of T, P_{O_2} and x. Two kinds of second phases, $SrCrO_4$ and an unknown phase, were observed depending on conditions. Both second phases tend to form at low T, in high P_{O_2} and with large Sr content, which is characteristic of the oxidation of Cr^{4+} in the solid solution to the higher valence. The solubility limit, x, for $La_{1-x}Sr_xCrO_3$ is much smaller than that for $La_{1-x}Ca_xCrO_3$; for example, under a typical operating condition of an SOFC cathode (1273 K, air), the values for Sr and Ca are approximately 0.1 and 0.3, respectively. For the application of $La_{1-x}Sr_xCrO_3$ to SOFC interconnectors, much attention should be paid to its narrow solubility range of Sr.

Acknowledgments

The authors acknowledge the financial support from the Ministry of Education, Culture, Science, Sports and Technology, Grant-in-Aid for Scientific Research (A), 13305046, 2002. Part of this study was also supported by NEDO of JAPAN.

References

[1] R.T. Baker, I.S. Metcalfe, Appl. Catal. A 126 (1995) 297.
[2] P. Vernoux, J. Guindet, M. Kleitz, J. Electrochem. Soc. 145 (1998) 3487.
[3] S. Primdahl, J.R. Hansen, L. Grahl-Madsen, P.H. Larsen, J. Electrochem. Soc. 148 (2001) A74.
[4] J.D. Carter, V. Sprenkle, M.M. Nasrallash, H.U. Anderson, in: S.C. Singhal, H. Iwahara (Eds.), Proceedings of the Third International Symposium on Solid Oxide Fuel Cells, PV 93-4, The Electrochemical Society Proceedings Series, Pennington, NJ, 1993, p. 344.
[5] D.H. Peck, M. Miller, K. Hilpert, Solid State Ion. 123 (1999) 47.
[6] D.H. Peck, M. Miller, K. Hilpert, Solid State Ion. 123 (1999) 59.
[7] H. Yokokawa, N. Sakai, T. Kawada, M. Dokiya, J. Electrochem. Soc. 138 (1991) 1018.
[8] S. Onuma, S. Miyoshi, K. Yashiro, A. Kaimai, K. Kawamura, Y. Nigara, T. Kawada, J. Mizusaki, N. Sakai, H. Yokokawa, J. Solid State Chem. 170 (2003) 68.
[9] J.D. Carter, C.C. Appel, M. Mogensen, J. Solid State Chem. 122 (1996) 407.
[10] N. Sakai, T. Kawada, H. Yokokawa, M. Dokiya, J. Ceram. Soc. Jpn. 101 (1993) 1195.
[11] G. Eriksson, E. Rosen, Chem. Scr. 8 (1975) 100.
[12] H. Yokokawa, H. Fujishige, S. Ujiie, M. Dokiya, J. Natl. Chem. Lab. Ind. 83 (Special issue) (1988) 1–26.
[13] M.U. Pechini, US Patent No. 3,330,697 (1967).
[14] J.P.R. de Villiers, J. Mathias, A. Muan, Trans. Inst. Min. Metall. Sec. C 96 (1987) C55.
[15] N. Sakai, T. Kawada, H. Yokokawa, H. Dokiya, I. Kojima, J. Am. Ceram. Soc. 76 (1993) 609.
[16] T. Negas, R.S. Roth, J. Res. Natl. Bur. Stand. Sec. A 73 (1969) 431.